tvst

Article

Plane-Wave Ultrasound Doppler of the Eye in Preeclampsia

Ronald H. Silverman[1], Raksha Urs[1], Ronald J. Wapner[2], and Srilaxmi Bearelly[1]

[1] Department of Ophthalmology, Columbia University Irving Medical Center, New York, NY, USA
[2] Department of Obstetrics and Gynecology, Columbia University Irving Medical Center, New York, NY, USA

Correspondence: Ronald H. Silverman, Department of Ophthalmology, Columbia University Irving Medical Center, 635 West 165th St., Research Annex Room 711, New York, NY 10032, USA. e-mail: rs3072@cumc.columbia.edu

Received: May 15, 2020
Accepted: August 3, 2020
Published: September 14, 2020

Keywords: preeclampsia; eye; plane-wave; ultrasound; blood-flow; Doppler

Citation: Silverman RH, Urs R, Wapner RJ, Bearelly S. Plane-wave ultrasound doppler of the eye in preeclampsia. Trans Vis Sci Tech. 2020;9(10):14, https://doi.org/10.1167/tvst.9.10.14

Purpose: Pre-eclampsia (PE) is a serious complication of pregnancy characterized by high blood pressure, proteinuria, compromised fetal blood supply, and potential organ damage. The superficial location of the eye makes it an ideal target for characterization hemodynamics. Our aim was to discern the impact of PE on ocular blood flow.

Methods: 18 MHz plane-wave ophthalmic ultrasound scanning was performed on subjects with PE (n = 26), chronic or gestational hypertension (n = 8), and normal controls (n = 19) within 72 hours of delivery. Duplicate three-second long scans of the posterior pole including the optic nerve were acquired at 6000 images/sec for evaluation of the central retinal artery and vein and the short posterior ciliary arteries. The choroid was scanned at 1000 images/sec. Doppler analysis provided values of pulsatile flow velocity and resistance indexes.

Results: End diastolic velocity was higher, and pulsatility and resistive indexes were significantly lower in the choroid, central retinal artery and short posterior ciliary arteries in PE than in controls. Blood pressure was elevated in PE with respect to controls and was negatively correlated with resistance.

Conclusions: Although vasoconstriction is considered characteristic of PE, we found reduced resistance in the orbital vessels and choroidal arterioles, implying vasodilation at this level. Future studies incorporating optical coherence tomography angiography for characterization of the retina and choriocapillaris in conjunction with plane-wave ultrasound scanning, particularly in late pregnancy, might address this conundrum.

Translational Relevance: Use of plane-wave ultrasound scanning for evaluation ocular blood flow in women at risk for PE may offer an avenue towards early detection and clinical intervention.

Introduction

Pre-eclampsia (PE) is a rapidly progressive multisystem disorder characterized by the acute onset of hypertension occurring usually after 20 weeks of gestation and frequently associated with proteinuria and edema. Severe manifestations include reduced organ perfusion secondary to vasospasm and activation of the coagulation cascade.[1] It affects 4% to 7% of pregnant women and is one of the most serious complications of pregnancy. Despite extensive research, the cause of PE remains elusive.[2]

PE is fundamentally a disease of the vasculature and is directly implicated in an array of major maternal morbidities and adverse perinatal outcomes. Women destined to develop PE have increased vascular reactivity well before they become symptomatic. Identification of high-risk patients is based on clinical history, especially prior PE, diabetes, renal disease, and chronic hypertension.[3]

Presymptomatic warning of an elevated risk for development of PE would be a valuable clinical tool. A marker for severe progression could be crucial to the life and health of both mother and child. Severe complications of PE account for approximately 63,000 maternal deaths annually worldwide, with mortality rates especially high in less developed countries.[4] In the United States, PE accounts for approximately 16% of all maternal deaths and risk of fetal death is highly elevated, especially for PE occurring in the preterm period.[5,6] Women suffering PE are also at risk for high blood pressure, stroke, heart and renal disease, and vascular dementia later in life.[7]

While the placenta might be regarded as the most intuitive target for vascular imaging for assessment of PE risk,[8] it is far less accessible to high-resolution imaging of the vasculature than is the eye, where the retinal microvasculature can be visualized optically. This is especially true given recent advances in ocular imaging, such as optical coherence tomography angiography (OCT-A). Whereas the placenta is poorly placed for routine, high-resolution imaging, the eye is superficial, has a rich retinal and choroidal vasculature, and can be imaged noninvasively in near-microscopic detail.

In ophthalmology, B-scan instruments generally consist of mechanically scanned single-element transducers. These emit a focused ultrasound beam, and images are produced by measurement of the probe orientation and range and amplitude of echoes. Ophthalmic B-scan instruments typically produce about 10 images/sec and provide no information on blood-flow.

Linear array probes are dominant in other clinical specialties. With electronic rather than mechanical scanning, scan rate is 10 times faster, and Doppler techniques can be used to produce color-flow images superimposing regions of flow over the gray-scale structural image. This technology, however, has made negligible impact in ophthalmology because such systems generally exceed Food and Drug Administration (FDA) guidelines[9] for ophthalmic intensity thresholds.

Plane-wave ultrasound scanning is a recent technologic advance that offers the advantages of linear arrays with compliance to FDA-guidelines.[10,11] In this imaging mode, all array elements emit at once to produce an unfocused wavefront. Echo data received by the many elements are then brought into focus by postprocessing using a "delay-and-sum" algorithm, which is the inverse of how element firings would be timed to produce a converging, focused beam. Because the plane-wave is unfocused on transmit, ultrasound intensity is substantially lower than when using a standard scanned, focused beam, and because there is no scanning (electronic or mechanical), the imaging rate can be ~1000 times faster than with a mechanically scanned probe. Given the two-way pulse/echo transit time of the eye, roughly 15,000 B-scan images can be acquired per second.

We developed plane-wave ultrasound scanning for imaging of the eye and reported imaging and measurement of blood-flow in the major vessels and choroid.[8,12]

In this study, we describe plane-wave ultrasound imaging and measurement of ocular blood-flow in 53 subjects scanned post-partum within 72 hours of delivery, 26 of whom had PE.

Methods

This research followed the tenets of the Declaration of Helsinki and was approved by the Columbia institutional review board. Informed consent was obtained after explanation of the nature and possible consequences of the study.

Subjects

Human subjects were classified by one investigator (RW) into one of four groups: normal controls (n = 19), mild PE (mPE) (n = 7), severe PE (sPE) (n = 19), and chronic or gestational hypertension (HTN) (n = 8) based on criteria summarized in Table 1.[13,14] Classifications were masked to investigators until ultrasound data analysis was complete.

Blood pressure (BP) was measured in the patient's room before and after the ultrasound examination. Systolic and diastolic BP, pulse rate in beats per minute (BPM) were recorded. Mean arterial pressure (MAP) was calculated as (2*diastolic + systolic)/3. Pulse pressure was calculated as systolic – diastolic and pulse ratio as diastolic/systolic.

A dilated fundus examination was not performed as part of this study.

Ultrasound System

A Verasonics (Kirkland, WA, USA) Vantage-128 research ultrasound engine was used with a Verasonics L22-14vXLF 18 MHz linear array probe. The probe has a 12.8-mm aperture and elevation focus of about 18 mm.

Imaging

Patients were transported to the Harkness Eye Institute for ultrasound examination. Ophthalmic plane-wave ultrasound scanning was performed within 72 hours of delivery by a single investigator (RHS). Scanning was performed through closed eyelids with the subject in a seated position. GenTeal (Alcon, Geneva, Switzerland) ocular lubricant was applied to the probe surface as an acoustic coupling agent. Scanning was performed with minimum pressure to the eyelid to enable visualization and measurement of flow. For assessment of the retrobulbar vessels, the scan was in a horizontal plane encompassing the optic nerve. For the choroid, scans were in a horizontal plane just superior to the optic nerve. The dimension of the scanned region was approximately 12.8 mm laterally by 8 mm axially. Duplicate scans were acquired on both eyes. The scanning procedure had a duration of approximately five to ten minutes per eye.

Table 1. Classification Criteria

Condition	Hypertension	And One or More:	Clinical Signs
HTN	>140 systolic or >90 diastolic	—	> 20 weeks pregnancy
mPE	>140 systolic or >90 diastolic	Proteinuria >0.3 g/24 hr Thrombocytopenia: platelet count <100,000/μL Renal insufficiency: serum creatinine >1.1 mg/dL	> 20 weeks pregnancy
sPE	>160 systolic or >110 diastolic	Thrombocytopenia: platelet count <100,000/μL Renal insufficiency: serum creatinine >1.1 mg/dL	> 20 weeks pregnancy One or more: • Central nervous system: severe headache, cortical blindness • Ocular: photopsia, scotoma, retinal vasospasm • Liver: enzymes • Respiratory

We developed MATLAB (The MathWorks, Inc., Natick, MA, USA) programs to control transmit and receive of all transducer elements, enabling transmission of plane waves at multiple angles. Echo data received by the linear-array transducer elements were quadrature sampled at 62.5 MHz at 14-bits per sample.

In real-time "flash Doppler" mode,[15] color-flow power Doppler was superimposed on grayscale plane-wave B-mode images. Although Doppler resolution and sensitivity are relatively modest in this mode, it allows identification of relevant ocular structures and flow, enabling orientation of the probe for data acquisition.

Once the probe was properly oriented, we acquired high-resolution data from the posterior pole for approximately three seconds at 6 kHz, compounding echo data from two angled transmissions at ±9°. At this acquisition rate, velocities of up to 140 mm/sec could be measured before reaching the alias limit. For choroidal "slow flow," 10 angles were compounded and acquired at 1 kHz.

Postprocessing

All post-processing was performed by one investigator (RU). The first stage of data processing consisted of beamforming and coherent addition of each batch of angled plane-waves to form compound images. The data were subsequently processed using a singular value decomposition (SVD) filter,[16] followed by a 10-Hz high-pass filter. The SVD filter exploits the different spatial coherence characteristics of bulk tissue motion caused by small movements of the eye or the hand-held probe versus blood flow, even when their velocities are comparable. The 10-Hz high-pass filter sets a threshold of ∼0.5 mm/sec for minimum detectable velocity and acts to improve distinction of flow from noise. These operations remove 'clutter', consisting of stationary or slow-moving tissue, leaving only blood-flow.

Spectrograms representing flow velocity as a function of time were generated from user-selected regions of interest: the central retinal artery (CRA), central retinal vein (CRV), short posterior ciliary arteries (SPCAs) and choroid. After application of phase unwrapping to the spectrogram to compensate for potential aliasing, the envelope of the spectrogram was automatically detected.[17] The peak systolic velocity (PSV), end diastolic velocity (EDV) and average velocity (V_{MEAN}) in two successive cardiac cycles were measured and the resistive index calculated as RI = (PSV-EDV)/PSV and pulsatility index as PI = (PSV-EDV)/V_{MEAN}. Velocity values were cosine-corrected based on vessel angle with respect to the ultrasound axis. Doppler parameters for each vessel in the duplicate scans were averaged before subsequent statistical analysis. Figures 1 and 2 illustrate imaging and spectrograms at the posterior pole and choroid, respectively.

Statistical Analysis

Statistical analysis was performed with IBM SPSS, Version 25 (IBM Corp., Armonk, NY). Means and standard deviations of systemic BP parameters and ultrasound-determined flow parameters were deter-

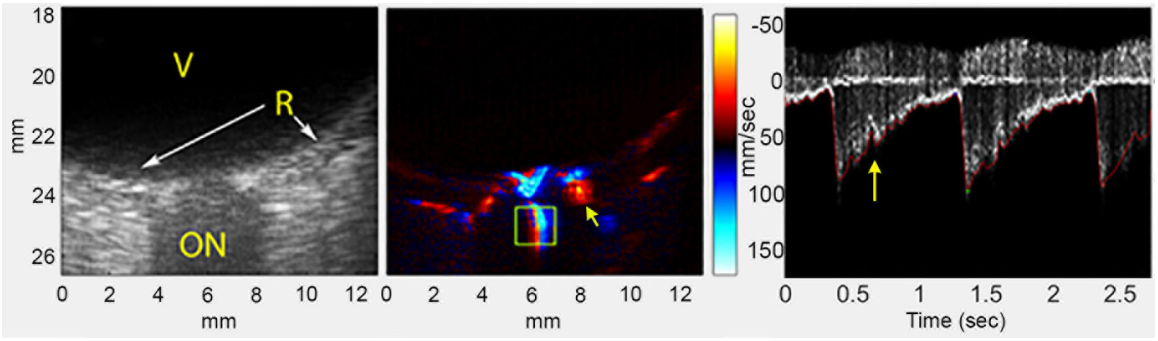

Figure 1. *Left*: B-mode plane-wave ultrasound image of posterior pole in normal subject. *Center*: High-resolution color flow Doppler image after processing of B-mode data, showing flow in central retinal artery (*red*) and vein (*blue*). *Arrow* indicates a short posterior ciliary artery. *Right*: Spectrogram demonstrating overlapping pulsatile flow from the central retinal artery (note dicrotic notch, *arrow*) and relatively nonpulsatile central retinal vein. V, vitreous; R, retina; ON, optic nerve.

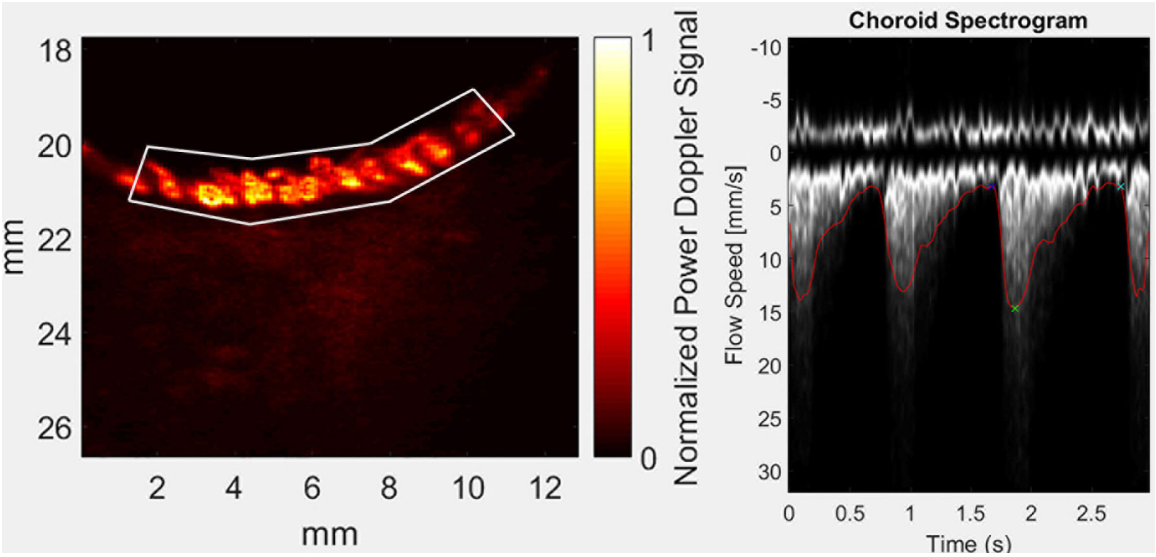

Figure 2. Representative power Doppler image (*left*) and spectrogram (*right*) of choroid from horizontal plane just superior to optic nerve head. The spectrogram is averaged over a large section of choroid as indicated by the boxed region superimposed on the Doppler image.

mined for each group and analysis of variance (ANOVA) performed. Correlation coefficients between BP and flow parameters were determined. Correlation coefficients for all measurements between left and right eyes were determined. Focusing specifically on sPE, we compared Doppler parameters in control versus sPE eyes by vessel using a general linear model (GLM) repeated measures procedure in which values from fellow eyes were treated as repeated measures to control for potential correlation between fellow eyes. Last, we repeated the GLM analysis with MAP as a covariate.

Results

Table 2 summarizes mean systemic parameters by diagnostic group. PE and HTN groups had higher BP than controls, but the diastolic/systolic ratio and heart rate were not significantly different.

Significant correlations between systemic BP and Doppler parameters (considering all groups together) are listed in Table 3. The table demonstrates significant correlations between systolic and diastolic BP and MAP with ocular flow parameters, particularly resistance (PE and RI). This was particularly notable in the sPE group, where diastolic BP had correlation coefficients of -0.562 and -0.529 with PI in the CRA and SPCA, respectively. This negative correlation was also evident to a lesser degree in control subjects.

We also examined Doppler parameters for correlation with the time interval between delivery and the ultrasound examination. ANOVA showed no significant difference in the time interval between groups. We found positive correlations between the interval and

Table 2. Systemic Blood Pressure Parameters (in mm Hg) and ANOVA by Group

DIAG		Systolic	Diastolic	Pulse Pressure	Ratio	MAP	BPM
Control (N = 19)	Mean	111.05	71.21	39.84	0.640	84.49	76.37
	SD	12.87	9.24	5.57	0.031	10.26	10.68
mPE (N = 7)	Mean	132.29	80.14	52.14	0.606	97.52	78.37
	SD	12.35	8.59	6.31	0.031	9.55	14.11
sPE (N = 19)	Mean	131.37	82.42	48.95	0.630	98.73	76.73
	SD	13.68	7.46	9.62	0.046	8.88	13.19
HTN N = 8	Mean	124.00	79.50	44.50	0.641	94.33	77.29
	SD	10.25	8.79	5.88	0.043	8.89	15.70
ANOVA							
F		9.50	5.98	6.95	1.54	7.98	0.45
P		<0.001	0.001	0.001	0.217	<0.001	0.716

Ratio, diasystolic/systolic; MAP, mean arterial pressure; BPM, beats/minute.

Table 3. Statistically Significant Correlations of Ocular Flow Velocity Parameters with Systemic Blood-Pressure Variables in the CRA, CRV, and SPCA

Systemic BP Variable	Vessel	Parameter	*R*	*P*
Systolic	CRA	PI	−0.353	0.010
	SPCA	RI	−0.321	0.019
	SPCA	PI	−0.357	0.009
	CRV	EDV	−0.306	0.039
Diastolic	CRA	RI	−0.314	0.022
	CRA	PI	−0.410	0.002
	SPCA	RI	−0.403	0.003
	SPCA	PI	−0.387	0.004
	CRV	EDV	−0.338	0.022
	CRV	Vmean	−0.293	0.048
Pulse pressure				
Ratio	SPCA	PSV	0.275	0.046
	SPCA	EDV	0.317	0.021
MAP	CRA	RI	−0.287	0.037
	CRA	PI	−0.397	0.003
	SPCA	RI	−0.379	0.005
	SPCA	PI	−0.386	0.004
	CRV	EDV	−0.335	0.023
	CRV	Vmean	−0.297	0.045

diastolic ($R = 0.346$, $P = 0.020$) and mean velocity ($R = 0.324$, $P = 0.030$), but only in the short posterior ciliary artery. We repeated the analysis for just the sPE group and found no significant correlation between Doppler parameters and time interval.

Mean Doppler parameters by group and their standard deviations are presented for each vessel in Tables 4 to 7. ANOVA shows significant differences among groups. EDV, V_{MEAN}, RI, and PI were all significant in the choroid. PI was significant in all vessels with exception of the CRV (which has negligible pulsatility).

Although there was a trend toward increased flow velocities in the HTN group compared with controls, this was not statistically significant. The low number of cases in this group, however, makes this a tentative finding.

Table 8 provides correlation coefficients between left and right eyes of each measurement. In most cases, correlation was small to moderate ($R < 0.5$), but all measurements were highly correlated ($R > 0.6$) in the SPCA. This is a surprising finding given the irregular directionality of the SPCAs but perhaps reflects greater averaging, because often more than one SPCA was imaged per scan.

GLM findings comparing Doppler parameters in control versus sPE eyes are presented in Table 9. Significant differences in EDV were found in the choroid and CRA, for V_{MEAN} in the CRA, and for RI and PI in all vessels other than the CRV. Table 10 repeats this analysis, but adding MAP as a covariate. When taking MAP into account, no variable attained statistical significance.

Discussion

From GLM comparison of controls with sPE and their means (shown in Tables 4–7), we find EDV to be significantly elevated in sPE with respect to controls in the choroid and CRA, and resistance indexes reduced. Resistance was also significantly reduced in the SPCA. These resistance indices were negatively correlated with BP parameters, particularly diastolic and mean arterial pressure.

Table 4. Choroidal Flow Velocity Parameters With ANOVA by Group

DIAG		PSV	EDV	V_{MEAN}	RI	PI
Control (N = 19)	Mean	9.580	4.160	6.019	0.528	0.870
	SD	2.056	0.813	1.095	0.105	0.268
mPE (N = 7)	Mean	9.088	3.660	5.415	0.549	0.956
	SD	2.528	0.896	1.222	0.0911	0.227
sPE (N = 19)	Mean	9.389	4.784	6.592	0.455	0.678
	SD	1.769	0.777	0.895	0.107	0.251
HTN (N = 8)	Mean	11.223	5.092	7.217	0.545	0.870
	SD	2.176	1.324	1.313	0.053	0.148
ANOVA						
	F	1.87	4.65	4.38	2.85	3.28
	P	0.148	0.006	0.008	0.047	0.029

Table 5. Central Retinal Artery Flow Velocity Parameters With ANOVA by Group

DIAG		PSV	EDV	V_{MEAN}	Resistive Index	Pulsatility Index
Control (N = 19)	Mean	75.701	9.502	28.009	0.869	2.586
	SD	18.825	5.222	9.585	0.057	0.669
mPE (N = 7)	Mean	87.403	12.026	39.087	0.862	2.061
	SD	31.351	6.611	17.171	0.048	0.443
sPE (N = 19)	Mean	83.407	14.237	37.882	0.819	1.974
	SD	19.163	6.362	10.644	0.063	0.531
HTN (N = 8)	Mean	75.955	13.285	35.143	0.827	1.960
	SD	20.540	12.369	14.113	0.108	0.480
ANOVA						
	F	.812	1.45	2.76	2.03	4.50
	p	0.493	0.240	0.052	0.122	0.007

Our findings are consistent with the observation of reduced vascular resistance in transcranial Doppler studies of the cerebral arteries of women with PE reported by Riskin-Mashiah et al.[18] and in the ophthalmic artery by Hata et al.[19,20] and Diniz et al.[21] Sato et al.[22] reported declining vascular resistance and an inverse correlation with MAP in the retinal vessels in late pregnancy in normal subjects using laser Doppler flowmetry. Alves Borges et al.[23] reported reduced resistance in the ophthalmic artery in post-partum PE versus control subjects. Belfort et al.,[24] however, reported that whereas resistance was negatively correlated with MAP in normal pregnancies, it was *positively* correlated with MAP in the CRA and ophthalmic artery in PE.

Our observation of decreased vascular resistance in PE and a negative correlation with BP are consistent with most of the above prior studies of cerebral, orbital, and retinal blood flow. It has been proposed that in PE, vascular hypertension and end-organ hyperperfusion are causal agents in tissue damage, e.g., proteinuria arising from kidney damage. It has been suggested that early-onset PE results from abnormal production of placental angiogenic proteins that, on entering the maternal circulation, disturb endothelial function[25] and that late-onset PE is a compensatory response to ongoing fetal metabolic demands surpassing the placenta's ability to sustain adequate fetal growth.[26] In either case, angiogenic factors in the maternal circulation induce reduced vascular resistance and elevated end-organ perfusion.

Vasospasm, however, has long been considered characteristic of PE onset and progression. In the case of the eye, this is supported by the narrowing of the retinal vessels in PE reported by Lupton et al.[27] and Soma-Pillay et al.[28] In both reports, however, retinal vessel caliber was corrected by dividing by MAP, which, given the elevated BP in PE, is a potentially confound-

Table 6. Short Posterior Ciliary Artery Flow Velocity Parameters With ANOVA by Group

DIAG		PSV	EDV	V_{MEAN}	RI	PI
Control (N = 19)	Mean	97.477	17.835	45.762	.823	1.931
	SD	36.623	12.494	21.032	.086	.517
mPE (N = 7)	Mean	112.068	21.045	54.879	.812	1.774
	SD	32.681	7.321	18.797	.053	.277
sPE (N = 19)	Mean	96.242	24.393	50.387	.749	1.547
	SD	28.825	12.523	17.726	.088	.388
HTN (N = 8)	Mean	92.774	22.996	52.234	.765	1.471
	SD	41.752	18.184	30.492	.06	.269
ANOVA						
	F	.471	.855	.398	3.09	3.69
	p	.704	.471	.755	.035	.018

Table 7. Central Retinal Vein Flow Velocity Parameters With ANOVA by Group

DIAG		PSV	EDV	V_{MEAN}	RI	PI
Control (N = 15)	Mean	−27.085	−13.466	−19.224	.490	.736
	SD	11.446	6.218	8.714	.134	.290
mPE (N = 6)	Mean	−37.001	−17.419	−25.847	.500	.741
	SD	18.190	6.641	11.325	.102	.215
sPE (N = 17)	Mean	−30.724	−18.449	−23.446	.392	.558
	SD	7.806	4.688	6.126	.141	.275
HTN (N = 8)	Mean	−27.947	−13.910	−20.450	.510	.742
	SD	11.165	8.025	9.227	.144	.275
ANOVA						
	F	1.22	2.19	1.25	2.21	1.57
	p	.316	.103	.305	.101	.211

Note that in some eyes the CRV was not visualized, so that N is less than the full cohort.

Table 8. Correlation Coefficients Between Right and Left Eye of Doppler Measurements by Vessel

	PSV	EDV	V_{MEAN}	RI	PI
Choroid	0.241	0.206	0.158	0.259	0.365*
CRA	0.314*	0.310*	0.432**	0.248	0.464**
CRV	0.427*	0.224	0.380*	0.189	0.288
SPCA	0.679**	0.603**	0.643**	0.650**	0.603**

*$P < 0.05$.
**$P < 0.01$.

Table 9. GLM of Doppler Parameters for Controls Versus sPE

	PSV	EDV	V_{MEAN}	RI	PI
Choroid					
F	0.094	**5.84**	3.12	**4.46**	**5.23**
P	0.761	**0.021**	0.086	**0.042**	**0.028**
CRA					
F	1.56	**6.29**	**9.03**	**6.47**	**9.74**
P	0.219	**0.017**	**0.005**	**0.015**	**0.004**
CRV					
F	0.123	1.56	0.542	1.76	1.16
P	0.730	0.228	0.471	0.201	0.296
SPCA					
F	0.039	2.20	0.335	**5.90**	**5.77**
P	0.845	0.147	0.567	**0.020**	**0.022**

Statistically significant differences are highlighted in bold.

ing procedure. In our own experience, (uncorrected) retinal vessel calibers were not significantly different between 35 control and 31 sPE subjects.[29]

Retinal vessel narrowing, if present, would seemingly be in contradiction with the reduced vascular resistance in the orbital vessels and choroid observed in this and most other studies. One explana-

Table 10. GLM of Doppler Parameters for Control Versus sPE Controlling for MAP

	PSV	EDV	V_{MEAN}	RI	PI
Choroid					
F	0.027	2.47	1.79	1.62	2.21
P	0.900	0.125	0.189	0.211	0.146
CRA					
F	0.558	1.16	2.94	1.24	2.45
P	0.460	0.290	0.095	0.272	0.127
CRV					
F	0.771	0.032	0.084	2.42	1.29
P	0.392	0.860	0.775	0.138	0.273
SPCA					
F	0.269	0.620	1.18	0.349	0.887
P	0.607	0.437	0.286	0.559	0.353

tory hypothesis is that overperfusion of the orbital vasculature causes the vessels of the choriocapillaris to become congested, resulting in retinal arteriolar vasospasm as a retinal defensive mechanism.[30] This is supported by our prior OCT observation of increased retinal and choroidal thickness in certain subsets of PE.[31,32] We hypothesized that that this subclinical edema might originate from changes in the Vascular Endothelial Growth Factor (VEGF)-sensitive choriocapillaris.[33] In the present study, we observed reduced resistance in the choroid. Note, however, that our plane-wave measurements pertain to the choroidal arterioles of Haller's and Sattler's layers rather than the choriocapillaris.[7]

A limitation of this study is that it was performed postpartum. However, although removal of the placenta is classically considered the cure for PE, it is well known that the vascular effects continue through the early and sometimes later postpartum period.

Another limitation is that Doppler measurements provide only velocity values rather than volumetric flow, which is very sensitive to lumen diameter changes. It has been shown that retinal arteriolar caliber tends to narrow as blood pressure increases, and that factors such as age, gender and smoking are significant covariates.[34,35] Our findings confirm systemic blood pressure to be an important covariate of ocular flow velocity parameters in PE. Because the present study was comprised of female subjects of childbearing age, gender and age are unlikely to be significant as covariates.

Vessel caliber is a crucial element affecting perfusion. Lumen diameters of the vessels interrogated in this study are not revealed by ultrasound. Hence, while flow velocity was measured, volumetric flow is unknown and potentially affected by changes in velocity, lumen diameter, or both. The lumens of the CRA, SPCA and CRV have been variously reported to range from about 0.1 to 0.2 mm.[36,37] Volumetric flow is determined by the pressure gradient between vessel input and outlet divided by resistance, which according to the Poiseuille equation, varies inversely with the fourth power of lumen diameter. Hence, a small change in diameter will result in a large change in flow. Assuming a constant pressure gradient, a 10% decrease in radius of the CRA or SPCA (just 5–10 µm) would result in a 36% decrease in volumetric flow to the retina or choroid, respectively.

Conclusions

In this study, we demonstrated the feasibility of imaging and measuring ocular blood flow in PE with plane-wave ultrasound scanning. We found significantly decreased flow resistance in sPE with respect to controls in the CRA, SPCA, and choroid. The seeming contradiction between our finding of decreased orbital and choroidal resistance with some reports of retinal vasoconstriction in PE might be addressed in future studies using ultrasound scanning in conjunction with OCT-A. Although OCT-A cannot at present measure flow dynamics, it has allowed demonstration of subtle structural changes in the retina[38] and choriocapillaris[39] in PE. Swept-source OCT-A is particularly adept in imaging and characterizing the choriocapillaris.[40] Measurement of vascular density, voids and lumen cross sections in the choriocapillaris together with ultrasound-determination of flow resistance in the choroid and orbital vessels would offer new insights regarding flow in the eye and, possibly, generally in end-organs in pregnancy and PE. Spectral domain OCT or adaptive optics measurement of retinal vessel wall thickness and lumen diameter[41,42] could also contribute to understanding ocular flow dynamic changes in PE.

Previous studies have shown that increased vascular reactivity occurs prior to the onset of PE, suggesting ophthalmic Doppler alterations could identify woman prior to the onset of clinical disease.[43] To unambiguously determine the potential of the technique to assess risk of developing PE, longitudinal imaging of pregnant woman before the onset of symptoms would allow elucidation of the development of altered ocular flow as a precursor to development of PE.

Acknowledgments

The authors thank Inez Nelson for her assistance in organizing data.

Supported by NIH Grants R01 EY025215, P30 EY019007 and National Center for Advancing Translational Sciences grant UL1TR001873, the New York Community Trust—Theresa Dow Wallace Fund and an unrestricted grant to Columbia Dept. of Ophthalmology from Research to Prevent Blindness. The content is solely the responsibility of the authors and does not necessarily represent the official views of the NIH.

Disclosure: **R.H. Silverman,** None; **R. Urs,** None; **R.J. Wapner,** None; **S. Bearelly,** None

References

1. Ananth CV, Keyes KM, Wapner RJ. Preeclampsia rates in the United States, 1980-2010: age-period-cohort analysis. *BMJ*. 2013;347:f6564.
2. Ness RB, Sibai BM. Shared and disparate components of the pathophysiologies of fetal growth restriction and preeclampsia. *Am J Obstet Gynecol*. 2006;195:40–49.
3. Copel JA, Platt LD, Hobbins JC, et al. Gottesfeld-Hohler Memorial Foundation Risk Assessment for Early-Onset Preeclampsia in the United States: think tank summary. *Obstet Gynecol*. 2020;135:36–45.
4. Vigil-De Gracia P. Maternal deaths due to eclampsia and HELLP syndrome. *Int J Gynaecol Obstet*. 2009;104:90–94.
5. Shih T, Peneva D, Xu X, et al. The rising burden of preeclampsia in the United States impacts both maternal and child health. *Am J Perinatol*. 2016;33:329–338.
6. Harmon QE, Huang L, Umbach DM, et al. Risk of fetal death with preeclampsia. *Obstet Gynecol*. 2015;12:628–635.
7. Jim B, Karumanchi A. Preeclampsia: pathogenesis, prevention, and long-term complications. *Semin Nephrol*. 2017;37:386–397.
8. Demers S, Boutin A, Dembickaja R, et al. Factors associated with placental vascularization measured by 3d power Doppler ultrasonographic sphere biopsy between 11 and 14 Weeks of Gestation. *Am J Perinatol*. 2018;35:964–971.
9. *Information for Manufacturers Seeking Marketing Clearance of Diagnostic Ultrasound Systems and Transducers*. Rockville, MD: Center for Devices and Radiological Health, Food and Drug Administration, US Department of Health and Human Services. 2008.
10. Tanter M, Fink M. Ultrafast imaging in biomedical ultrasound. *IEEE Trans Ultrason Ferroelectr Freq Control*. 2014;61:102–119.
11. Urs R, Ketterling JA, Silverman RH. Ultrafast ultrasound imaging of ocular anatomy and blood flow. *Invest Ophthalmol Vis Sci*. 2016;57:3810–3816.
12. Urs R, Ketterling JA, Yu ACH, Lloyd HO, Yiu BYS, Silverman RH. Ultrasound imaging and measurement of choroidal blood flow. *Transl Vis Sci Technol*. 2018;7:1–8.
13. Report of the National High Blood Pressure Education Program Working Group on High Blood Pressure in Pregnancy. *Am J Obstet Gynecol*. 2000;183:S1–S22.
14. American College of Obstetricians and Gynecologists (ACOG). Practice Bulletin No. 222: Gestational hypertension and preeclampsia. *Obstet Gynecol*. 2020;135:e237–e260.
15. Flynn J, Daigle R, Pflugrath L, Kaczkowski P. High frame rate vector velocity blood flow imaging using a single plane wave transmission angle. *Proc IEEE Int Ultrason Symp*. 2012;323–325.
16. Demene C, Deffieux T, Pernot M, et al. Spatiotemporal clutter filtering of ultrafast ultrasound data highly increases Doppler and fUltrasound sensitivity. *IEEE Trans Med Imaging*. 2015;34:2271–2285.
17. Kathpalia A, Karabiyik Y, Simensen B, et al. A robust Doppler spectral envelope detection technique for automated blood flow measurements. Proc IEEE Int Ultrason Symp. 2015;1–4.
18. Riskin-Mashiah SR, Belfort MA, Saade GR, et al. Transcranial Doppler measurement of cerebral velocity indices as a predictor of preeclampsia. *Am J Obstet Gynecol*. 2002;187:1667–1672.
19. Hata T, Senoh D, Hata K, et al. Ophthalmic artery velocimetry in preeclampsia. *Gynecol Obstet Invest*. 1995;40:32–35.
20. Hata T, Hata K, Moritake K. Maternal ophthalmic artery Doppler velocimetry in normotensive pregnancies and pregnancies complicated by hypertensive disorders. *Am J Obstet Gynecol*. 1997;177:174–178.
21. Diniz AL, Moron AF, Santos MC, et al. Ophthalmic artery Doppler as a measure of severe preeclampsia. *Int J Gynaecol Obstet*. 2008;100:216–220.
22. Sato T, Dugawara J, Aizawa N, et al. Longitudinal changes of ocular blood flow using laser speckle

flowgraphy during normal pregnancy. *PLoS One*. 2017;12:e0173127.
23. Alves Borges JH, Goes DA, de Araújo LB, et al. Prospective study of the hemodynamic behavior of ophthalmic arteries in postpartum preeclamptic women: A Doppler evaluation. *Hypertens Pregnancy*. 2016;35:100–111.
24. Belfort M, Saade GR, Grunewald C, et al. Effects of blood pressure on orbital and middle cerebral artery resistances in healthy pregnant women and women with preeclampsia. *Am J Obstet Gynecol*. 1999;180:601–607.
25. Karumanchi SA. Angiogenic factors in preeclampsia: from diagnosis to therapy. *Hypertension*. 2016;67:1072–1079.
26. Espinoza J, Uckele JE, Starr RA, et al. Angiogenic imbalances: the obstetric perspective. *Am J Obstet Gynecol*. 2010;203:17.e1–17.e8.
27. Lupton SJ, Chiu CL, Hodgson LAB, et al. Changes in retinal microvascular caliber precede the clinical onset of preeclampsia. *Hypertension*. 2013;62:899–904.
28. Soma-Pillay P, Pillay R, Wong TY, et al. The effect of pre-eclampsia on retinal microvascular caliber at delivery and post-partum. *Obst Med*. 2018;11:116–120.
29. Ciccone L, Lee W, Ananth CV, et al. Retinal vessel caliber measurements do not differ between severe preeclampsia and normotensive controls in the immediate post-partum period. Presented at Women in Ophthalmology, August 16-19, 2018, Ponte VedraBeach, FL.
30. Barbosa A, Cabral A, Reis Z. The association between retinal detachment in severe preeclampsia and blood flow parameters in ophthalmic and central retinal arteries on ecodoppler. *Hypertens in Preg*. 2004;23:91.
31. Garg A, Wapner RJ, Ananth CV, et al. Choroidal and retinal thickening in severe preeclampsia. *Invest Ophthalmol Vis Sci*. 2014;55:5723–5729.
32. Stern-Ascher CN, North VS, Garg A, Ananth CV, Wapner RJ, Bearelly S. Subfoveal choroidal thickness and associated changes of angiogenic factors in women with severe preeclampsia. [e-pub ahead of print]. *Am J Perinatol*. 2019, doi:10.1055/s-0039-1698832.
33. Blaauwgeers HG, Holtkamp GM, Rutten H, et al. Polarized vascular endothelial growth factor secretion by human retinal pigment epithelium and localization of vascular endothelial growth factor receptors on the inner choriocapillaris: evidence for a trophic paracrine relation. *Am J Pathol*. 1999;155:421–428.
34. Dervenis N, Coleman AL, Harris A, et al. Factors associated with retinal vessel diameters in an elderly population: the Thessaloniki Eye Study. *Invest Ophthalmol Vis Sci*. 2019;60:2208–2217.
35. Hubbard LD, Brothers RJ, King WN, et al. Methods for evaluation of retinal microvascular abnormalities associated with hypertension/sclerosis in the Atherosclerosis Risk in Communities Study. *Ophthalmology*. 1999;106:2269–2280.
36. Rim TH, Choi YS, Kim SS, et al. Retinal vessel structure measurement using spectral-domain optical coherence tomography. *Eye (Lond)*. 2016;30:111–119.
37. Wiącek MP, Modrzejewska M, Zaborski D. Age-related changes in retrobulbar circulation: a literature review. *Int Ophthalmol*. 2020;40:493–501.
38. Ciloglu E, Okcu NT, Dogan NC. Optical coherence tomography angiography findings in preeclampsia. *Eye*. 2019;33:1946–1951.
39. Urfalıoglu S, Bakacak M, Özdemir G, et al. Posterior ocular blood flow in preeclamptic patients evaluated with optical coherence tomography angiography. *Pregnancy Hypertens*. 2019;17:203–208.
40. Zhang Q, Zheng F, Motulsky EH, et al. A novel strategy for quantifying choriocapillaris flow voids using swept-source OCT Angiography. *Invest Ophthalmol Vis Sci*. 2018;59:203–211.
41. Muraoka Y, Tsujikawa A, Kumagai K, et al. Age- and hypertension-dependent changes in retinal vessel diameter and wall thickness: an optical coherence tomography study. *Am J Ophthalmol*. 2013;156:706–714.
42. Streese L, Brawand LY, Gugleta K, et al. New frontiers in noninvasive analysis of retinal wall-to-lumen ratio by retinal vessel wall analysis. Transl Vis Sci Technol. 2020;9:7.
43. Spaan JJ, Brown MA. Renin-angiotensin system in pre-eclampsia: everything old is new again. *Obstet Med*. 2012;5:147–153.